



Original Article

Calibration-free real-time organic film thickness monitoring technique by reflected X-Ray fluorescence and Compton scattering measurement



Junghwan Park ^{a, b}, Yong Suk Choi ^a, Junhyuck Kim ^{a, ***}, Jeongmook Lee ^a, Tae Jun Kim ^a, Young-Sang Youn ^c, Sang Ho Lim ^{a, d, **}, Jong-Yun Kim ^{a, d, *}

^a Nuclear Chemistry Research Team, Korea Atomic Energy Research Institute, 111, Daedeok-daero 989beon-gil, Yuseong-gu, Daejeon, 34057, Republic of Korea

^b Department of Nuclear and Quantum Engineering, Korea Advanced Institute of Science and Technology, 291 Daehak-ro, Yuseong-gu, Daejeon, 34141, Republic of Korea

^c Department of Chemistry, Yeungnam University, Daehak-ro 280, Gyeongsan, Gyeongbuk, 38541, Republic of Korea

^d Radiochemistry & Nuclear Nonproliferation, University of Science & Technology, Gajeong-ro 217, Yuseong-gu, Daejeon, 34113, Republic of Korea

ARTICLE INFO

Article history:

Received 10 July 2020

Received in revised form

31 August 2020

Accepted 14 September 2020

Available online 17 September 2020

Keywords:

Organic film

X-ray fluorescence

Compton scattering

X-ray radiation

Thickness

ABSTRACT

Most thickness measurement techniques using X-ray radiation are unsuitable in field processes involving fast-moving organic films. Herein, we propose a Compton scattering X-ray radiation method, which probes the light elements in organic materials, and a new simple, non-destructive, and non-contact calibration-free real-time film thickness measurement technique by setting up a bench-top X-ray thickness measurement system simulating a field process dealing with thin flexible organic films. The use of X-ray fluorescence and Compton scattering X-ray radiation reflectance signals from films in close contact with a roller produced accurate thickness measurements. In a high-thickness range, the contribution of X-ray fluorescence is negligible, whereas that of Compton scattering is negligible in a low-thickness range. X-ray fluorescence and Compton scattering show good correlations with the organic film thickness ($R^2 = 0.997$ and 0.999 for X-ray fluorescence and Compton scattering, respectively, in the thickness range 0–0.5 mm). Although the sensitivity of X-ray fluorescence is approximately 4.6 times higher than that of Compton scattering, Compton scattering signals are useful for thick films (e.g., thicker than ca. 1–5 mm under our present experiment conditions). Thus, successful calibration-free thickness monitoring is possible for fast-moving films, as demonstrated in our experiments.

© 2020 Korean Nuclear Society, Published by Elsevier Korea LLC. This is an open access article under the CC BY-NC-ND license (<http://creativecommons.org/licenses/by-nc-nd/4.0/>).

1. Introduction

Process analytical technology (PAT) is an emerging field in the quality control of many industrial processes [1–3]. PAT aims for an

effective and efficient quality management of raw, intermediate, and final products, which are key to success in modern industries for economic benefit, sampling procedure, transportation of samples, operational efficiency, and operational safety [4]. For a timely process control, an in-situ and real-time analysis for early fault detection is crucial in modern industrial processes [5]. Organic films have been used in various industries, such as electronic components with organic thin film transistors and solar cells [6–8]. Thickness is a major factor controlling the property and performance of an electronic product [9–11]. In spite of the high demands for monitoring film thickness, the relevant researches only dealt with inorganic film using X-ray scattering, absorption, fluorescence, and photoelectron emission [12–16]. To the best of our knowledge, there have been no practical method of real-time monitoring techniques based on X-ray technique to detect abrupt

* Corresponding author. Nuclear Chemistry Research Team, Korea Atomic Energy Research Institute, 111, Daedeok-daero 989beon-gil, Yuseong-gu, Daejeon, 34057, Republic of Korea.

** Corresponding author. Nuclear Chemistry Research Team, Korea Atomic Energy Research Institute, 111, Daedeok-daero 989beon-gil, Yuseong-gu, Daejeon, 34057, Republic of Korea.

*** Corresponding author. Nuclear Chemistry Research Team, Korea Atomic Energy Research Institute, 111, Daedeok-daero 989beon-gil, Yuseong-gu, Daejeon, 34057, Republic of Korea.

E-mail addresses: jhkim98765@kaeri.re.kr (J. Kim), slim@kaeri.re.kr (S.H. Lim), kjy@kaeri.re.kr (J.-Y. Kim).

changes in the thickness of films made of organic materials moving between rollers. There was a report on the measurement technique using ultraviolet light [17]. In our previous studies, we have proposed techniques using Compton scattering for measuring light elements in organic and inorganic materials [18,19]. However, we have measured the thickness of stationary organic films attached onto a solid metal substrate without any movement during measurements.

In real field processes dealing with thin flexible films, accurate measurements using X-ray transmission techniques are hindered by the fluctuation of films moving between rollers. Accordingly, the use of X-ray reflectance signals from films in close contact with a roller is proposed to provide accurate thickness measurement. In this study, X-ray fluorescence signals from a roller made of metal and reflected X-ray Compton scattering signals were used to measure the thickness of organic films composed of light elements, such as carbon and hydrogen. Based on our previous study on thickness measurement [19], we designed a bench-top X-ray monitoring system. For the simulation of industrial processes, the thickness of organic polymer films, as representative samples, on a moving roller was monitored in real time without performing calibration with standard samples.

2. Experimental methods

The in-house designed X-ray analysis system is shown in Fig. 1, and a geometric arrangement of the X-ray source, detector, and film on the roller is depicted in Fig. 2. Our film thickness measurement system consists of an X-ray tube (Mini-X-Ag, AMPTEK, USA) as an X-ray source, a cadmium telluride (CdTe) X-ray detector combined with a multi-channel analyzer (X-123-CdTe, AMPTEK, USA), and a rolling machine for the film sample. An X-ray tube generator includes a silver (Ag) target X-ray tube operating at 10–40 kV tube voltage, 5–200 μ A tube current, and 4 W maximum continuous power. The characteristic X-rays were mostly emitted from the Ag target, have energies of 22 keV (K_{α}) and 25 keV (K_{β}) [20], and have K_{α} emission with even greater intensity. The detector has about 100% intrinsic efficiency in the energy range of 10–60 KeV with a count rate of up to 2×10^5 count per second (cps) [21].

Three rollers are made of SUS 303 (71.97% Fe, 17.07% Cr, 8.94% Ni, and other elements), as confirmed by a handheld X-ray fluorescent

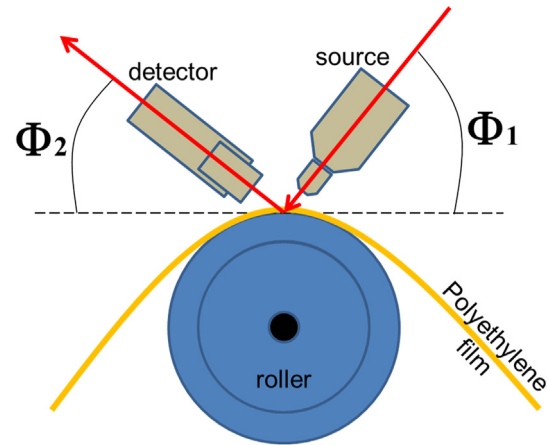


Fig. 2. Schematic of the geometric arrangement of the X-ray source, detector, and film on a roller. Φ_1 and Φ_2 are the angles of incident and scattered X-rays, respectively.

(XRF) analyzer (Delta DP2000, Innov-X, USA). Polyethylene film was used as a base film mounted on the rollers. The thickness of the polyethylene film was approximately 70 μ m per layer. In a stationary experiment (i.e., no movement of the films), the measurement conditions and dynamic range of the measurements were investigated by adjusting the angles of incident (Φ_1) and scattered (Φ_2) X-rays, as shown in Fig. 2, and manually increasing the thickness of the polyethylene films stacked layer by layer. The thickness of the polyethylene films increased to ca. 5 mm. Films thicker than 5 mm were not tested, because such a feature is beyond the scope of this study. In dynamic monitoring experiments for films moving from roller to roller using the rolling machine, a Fisherbrand adhesive tape purchased from Fisher Scientific was used to monitor abrupt changes in the film thickness, as shown in Fig. 1 (c). The adhesive tape thickness of each layer was ca. 160 μ m as measured with a field emission scanning electron microscope, and the tape was made of mostly light elements, such as carbon, as measured with an energy-dispersive X-ray spectrum (Supplementary data). The 2-cm-wide adhesive tape was cut into pieces, and several strips of the tape were placed onto the polyethylene base film with a distance of approximately 2 cm between the strips. The rollers were

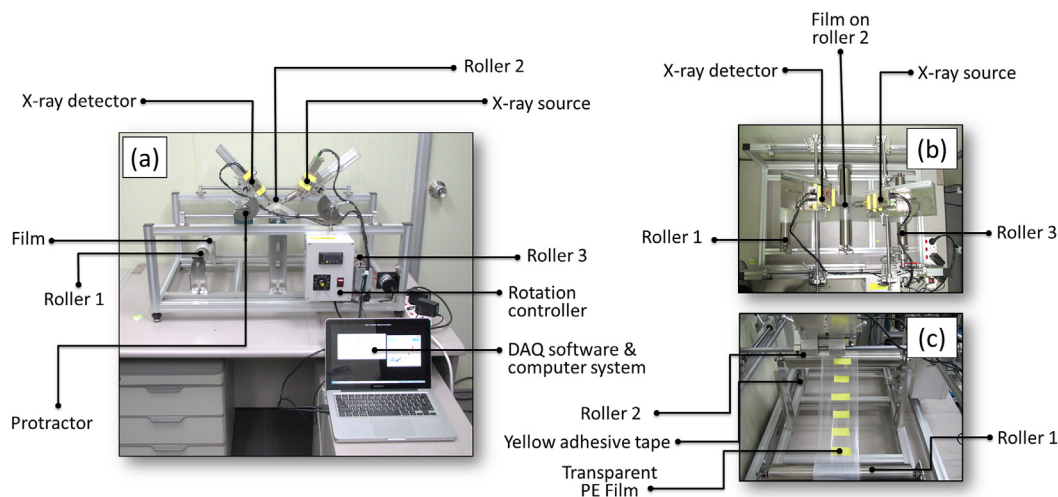


Fig. 1. On-line real-time thickness monitoring system. (a) Full view of the X-ray measurement system, including a roller machine and a data acquisition system, (b) top view and (c) side view of the yellow adhesive tapes placed on the transparent polyethylene film mounted on the roller. (For interpretation of the references to colour in this figure legend, the reader is referred to the Web version of this article.)

operated at a constant linear velocity of 50 or 150 cm min⁻¹ by a rotation controller to examine the effect of speed of the film movement on a roller. The detected scattered and fluorescence signals were obtained and processed with a data acquisition software (DppMCA, AMPTTEK, USA). The counting time at each channel was 0.1 s in every measurement, including the real-time monitoring experiments.

As the peak energy information is a critical factor in this study, 1024-channel CdTe was not energy calibrated similar with a previous study [22], and this study focuses on the qualitative calibration-free measurement technique. Instead, the integrated count rates, over the entire range of the channels or relative variation of the peak count rates by X-ray fluorescence and Compton scattering radiation, were used to monitor the relative thickness changes. The relative variations of the peak count rates were obtained by integrating the peak area under the curve for the channel number between 100–200 and 400–500, corresponding to the X-ray fluorescence and Compton scattered radiation signals in X-ray spectra, respectively.

3. Results and discussion

The use of Compton scattering signal was first proposed by van Sprang and Bekkers to quantify light elements [23]. One of the representative examples of the application of Compton scattering radiation is the determination of moisture content trapped in inorganic oxide pores [19]. The determination of thickness of films made of organic materials using the relation between the Compton scattering intensity (I_{Comp}) and film thickness (d) is an another example [19]:

$$I_{Comp} = \frac{\Omega \sigma I_0}{\mu' + \mu \sin \Phi_1 / \sin \Phi_2} \left[1 - \exp \left\{ -\rho d \left(\frac{\mu}{\sin \Phi_1} \frac{\mu'}{\sin \Phi_2} \right) \right\} \right], \quad (1)$$

$$I_{Comp} = A \{ 1 - \exp(-Bd) \}, \quad (2)$$

where Ω is the solid angle (steradian) of the detector, σ is the differential mass scattering coefficient (cm²/g per steradian) of Compton scattering, I_0 is the intensity of the incident X-ray, μ' is the mass absorption coefficient (cm²/g) of the sample at the Compton wavelength, μ is the mass absorption coefficient (cm²/g) of the sample at the incident wavelength, ρ is the density (g/cm³) of the films, d is the thickness (cm) of the organic film, Φ_1 is the angles between the incident X-rays and sample, and Φ_2 is the angles between scattered X-rays and sample. Eq. (1) is simplified into Eq. (2) with proportionality constants A and B of the other geometrical factors of the system and material properties, such that I_0 , σ , Ω , Φ_1 , Φ_2 , ρ , μ , and μ' are fixed and I_{Comp} increases with film thickness (d) only.

$$I_{fluor} = A' \times \exp(-B'd). \quad (3)$$

The attenuation of fluorescence intensity (I_{fluor}) by the organic films on the substrate can also be expressed by a simplified Eq. (3) with proportionality constants A' and B' . Fluorescence signals decrease with the film thickness.

To examine the sensitivity of the signals using the geometry of the system, the X-ray reflectance spectra of the polyethylene films with thicknesses varying from 0 to 5 mm were measured on a stationary roller at rest. Fig. 3 shows the effects of film thickness on the stationary roller at rest and scattered angle (Φ_2) at a fixed $\Phi_1 = 60^\circ$ on the responses of the X-ray detector. Two distinct peaks were detected. The peak intensity of the first peak decreased, whereas the second peak intensity increased, as the film thickness

increased from 0 to 5 mm. The X-ray fluorescence radiation from the stainless steel roller was attenuated by the film, as shown in Eq. (3), whereas the Compton scattering intensity was enhanced by the organic polyethylene film, as shown in Eq. (2). Thus, the first peak in Fig. 3 represents the X-ray fluorescence attenuation signal from the roller, and the second peak is the Compton scattering signal enhanced by the film. No significant effect of scattered angles was observed on the count rates under our current experimental conditions. Therefore, only the experimental results at 40° were shown for the following experiments, although some experiments were also performed at 60° to determine any unexpected effect on the results.

Fig. 4 shows the total count rate integrated over the entire channel range in Fig. 3 as a function of the polyethylene film thickness. The total count rates rapidly decreased as the film thickness increased up to approximately 3 mm and then slowly increased as the thickness further increased to 5 mm. The majority of the total count rates were derived from the sum of the X-ray fluorescence (first main peak in Fig. 3) and Compton scattering (second peak in Fig. 3) signals. The count rates of X-ray fluorescence and Compton scattering signals were obtained by integrating the peak area under the curve in Fig. 3 for the channel number between 100 and 200 and between 400 and 500, respectively. The initial rapid decrease and later gradual increase in the total sum of the count rates can be explained by the respective contribution of the X-ray fluorescence and Compton scattering. The correlations of X-ray fluorescence and Compton scattering signals with the thickness of the polyethylene film on a roller at rest are shown in Figs. 5 and 6, respectively. The initial rapid decrease of the total count rates in Fig. 4 is mainly caused by the attenuation of X-ray fluorescence by the organic films, where signals by Compton scattering are negligible in such a lower thickness range. Most of the signals were derived from X-ray fluorescence in a lower thickness range. However, they rapidly decreased with the film thickness, as shown in Fig. 5 (a), whereas Compton scattering radiation gradually increased, contributing to the total count rate more significantly as the thickness increased, as shown in Fig. 6 (a).

Regarding the X-ray fluorescence signals with film thickness, the exponential function represents the total count rate–thickness curve, presented in Fig. 5 (a), over the entire range of the film thickness. The coefficient of determination (R^2) of the X-ray fluorescence curves was 0.994. However, in a lower thickness range (up to ca. 0.5 mm), the count rate–thickness curve showed strong negative linear relations, where R^2 for $\Phi_2 = 40^\circ$ and $\Phi_2 = 60^\circ$ are 0.997 and 0.998, respectively, as shown in Fig. 5 (b). X-ray fluorescence signals were very sensitive to the film thickness in films thinner than ca. 0.5 mm. The sensitivities of the X-ray fluorescence signals with thickness were 43.0 and 53.1 kcps · mm⁻¹ for $\Phi_2 = 40^\circ$ and $\Phi_2 = 60^\circ$, respectively. However, the sensitivity of measurement is actually the slope of the curve in Fig. 5 (a), and it decreased with the film thickness, since the fluorescence intensity decreased exponentially according to Eq. (3). The limit of detection (LOD) and limit of quantification (LOQ) were also evaluated based on the sensitivity and standard error of mean with thickness of 0.1 mm, as shown in Fig. 5 (b). The LODs of the thickness measurement adopting fluorescence signals were 0.04 and 0.05 mm and the LOQs were 0.14 and 0.15 mm for $\Phi_2 = 40^\circ$ and $\Phi_2 = 60^\circ$, respectively.

The Compton scattering had a strong positive linear correlation over the entire range of the film thickness presented in Fig. 6 (a) unlike the fluorescence curve in Fig. 5 (a). In a higher thickness range, the signals from the Compton scattering became dominant in the total count rates and more sensitive to the thickness. R^2 of the linear count rate–thickness curves in Fig. 6 (a) and (b) was 0.999 for the entire thickness range of 0–5 mm and 0.995 for the thickness range of 0–0.5 mm, respectively. The sensitivity of Compton

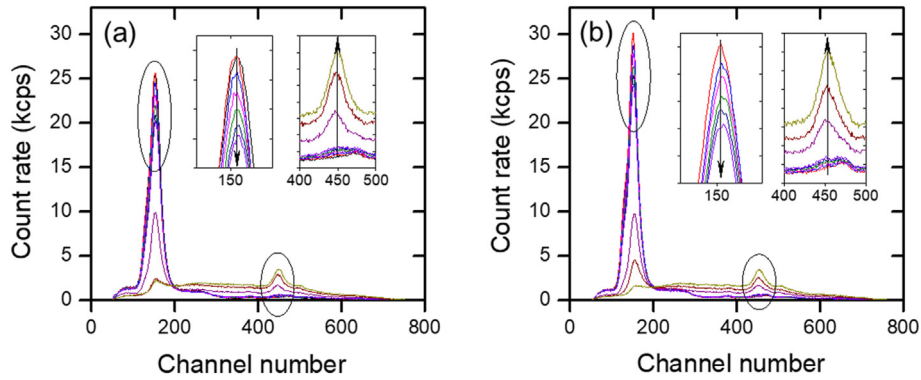


Fig. 3. X-ray reflectance spectra of the polyethylene film on a stainless steel roller at rest measured at scattered angles (Φ_2 in Fig. 2) of (a) 40° and (b) 60° , respectively, at $\Phi_1 = 60^\circ$. Thickness of the film on a roller varied from 0 mm to 5 mm. The two insets are the enlarged view of the curves in the range represented by the ellipsoidal line. Arrows indicate the direction of the thickness increment.

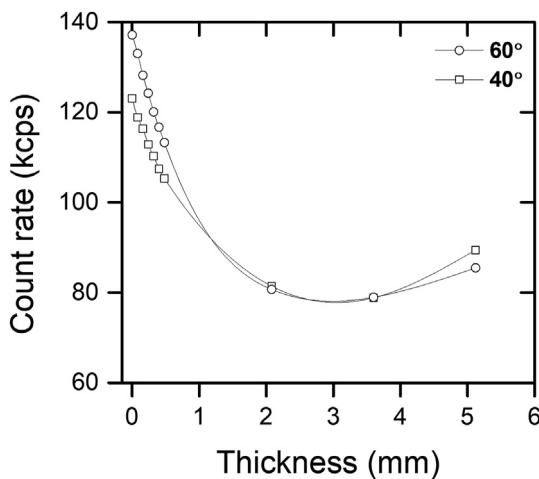


Fig. 4. Effect of scattered angle (Φ_2) and film thickness on the total count rates integrated over the whole range of X-ray spectra shown in Fig. 3. Diamonds and rectangular symbols denote the total count rates measured at $\Phi_2 = 40^\circ$ and 60° , respectively, for the stationary polyethylene film on a roller at rest. Φ_1 was fixed at 60° .

scattering was $3.8 \text{ kcps} \cdot \text{mm}^{-1}$. In terms of sensitivity, the X-ray fluorescence signal is significantly better than Compton scattering signal for accurately measuring the micrometer-thick films under

our current experimental conditions. However, unlike X-ray fluorescence, the Compton scattering signal showed excellent simple linear correlations even with film thickness up to 5 mm. This strong positive correlation between the thickness of organic films and Compton scattering is consistent with our previous study [19], and it suggests that X-ray Compton scattering is useful for the quantitative thickness determination of thick organic films. The sensitivities of the Compton scattering signals with thickness were 3.9 and $4.0 \text{ kcps} \cdot \text{mm}^{-1}$ for $\Phi_2 = 40^\circ$ and 60° , respectively. The LOD and LOQ calculated from Fig. 6 (b) based on the sensitivity and standard error of mean with thickness of 0.1 mm were 0.14 and 0.15 mm and the LOQs were 0.46 and 0.51 mm for $\Phi_2 = 40^\circ$ and 60° , respectively.

As roller machines are used to transport films in many processes, the X-ray reflectance spectra of the polyethylene films moving at a constant speed were investigated. The effect of film movement on the measurement accuracy was examined based on the results of previous experiments with films on a roller at rest, as shown in Figs. 3–6. Fig. 7 shows a linear relation of X-ray fluorescence and Compton scattering signals with the thickness of polyethylene film on a rotating roller at two different rotation speeds. The strong linear dependence with an increase in film thickness shown in Fig. 7 is consistent with the experimental results with the stationary roller at rest in Figs. 5 and 6, which indicates that the results from the acquisition of X-ray spectra of the moving film in the system are as reliable as those of the film at

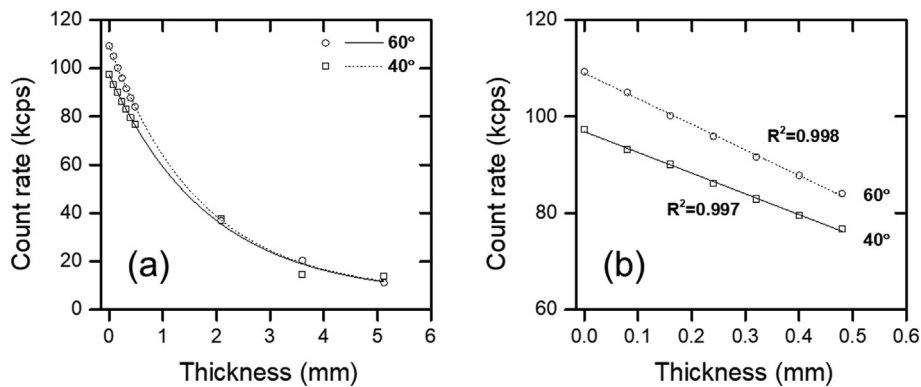


Fig. 5. Correlations of X-ray fluorescence signals with the thickness of the polyethylene film on a roller at rest. Count rate–film thickness curves showing (a) the entire thickness range, and (b) enlarged view of the curve in the thickness range $0\text{--}0.5 \text{ mm}$. Count rates in this figure were obtained by integrating the peak area under the curve in Fig. 3 for the channel number between 100 and 200 representing the X-ray fluorescence signals. Rectangular and circular symbols denote the total count rates measured at $\Phi_2 = 40^\circ$ and 60° , respectively, for the stationary polyethylene film on a roller at rest. Φ_1 was fixed at 60° .

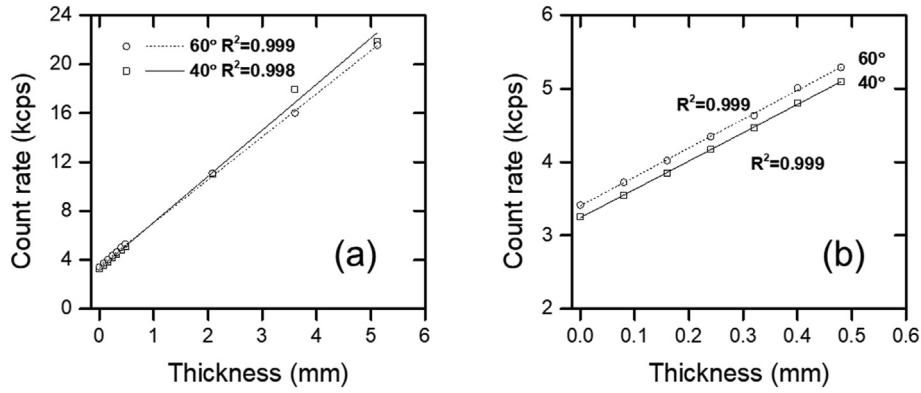


Fig. 6. Correlations of Compton scattering signals with the thickness of polyethylene film on a roller at rest. Count rate–film thickness curves showing (a) the entire thickness range, and (b) enlarged view of the curve in the thickness range 0–0.5 mm. Count rates in this figure were obtained by integrating the peak area under the curve in Fig. 3 for the channel number between 400 and 500 representing the Compton scattering signals. Rectangular and circular symbols denote the total count rates measured at $\Phi_2 = 40^\circ$ and 60° , respectively, for the stationary polyethylene film on a roller at rest. Φ_1 was fixed at 60° .

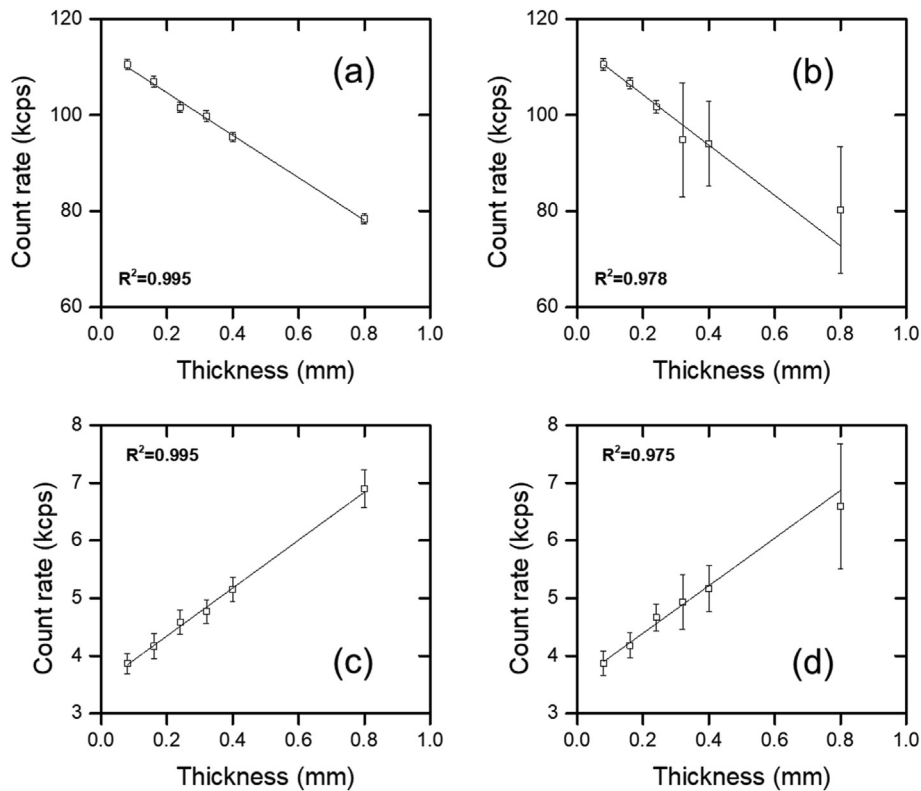


Fig. 7. Correlations of X-ray fluorescence signals or Compton scattering with the thickness of moving polyethylene film on a rotating roller. Count rates were obtained by integrating the peak area under the curve in Fig. 3 in the channel number between 100 and 200 for X-ray fluorescence signals and between 400 and 500 for Compton scattering signals, respectively, at $\Phi_1 = 60^\circ$ and $\Phi_2 = 60^\circ$. (a) and (b) curves are produced with the X-ray fluorescence signals, whereas (c) and (d) are produced with the Compton scattering signals. (a) and (c) are the data measured at a speed of 50 cm min^{-1} , whereas (b) and (d) are the data measured at a speed of 150 cm min^{-1} . Error bars represent the standard deviation of 100 measurements.

rest. The sensitivities presented in Fig. 7 (a)–(d) are 44.3, 52.5, 4.2, and $4.1 \text{ kcps} \cdot \text{mm}^{-1}$. As expected, sensitivity values are comparable to those of a stationary roller at rest. The LODs in Fig. 7 (a)–(d) were 0.08, 0.07, 0.13, and 0.15 mm, whereas the LOQs were 0.25, 0.22, 0.43, and 0.51 mm, all of which are also comparable to those of a stationary roller at rest. The linear velocity of the films did not significantly influence the sensitivity. However, the relatively large deviation of the count rates due to the rotation of the roller deteriorated the R^2 of the curve from 0.995 to 0.978 for the fluorescence signals and from 0.995 to 0.975 for the Compton

scattering signals, respectively, as the rotation speed of the rollers increased from 50 cm min^{-1} to 150 cm min^{-1} , except that shown in Fig. 7 (a), which exhibits the excellent linearity of the curve and a very small deviation of the count rate even as the thickness increased. The large variation in the count rate with the thickness and linear velocity of the film resulted from the fluctuation of the film layers because the films were stacked to prepare a thicker film sample without using any adhesives between layers. For example, to prepare 0.8 mm-thick samples, at least 10 layers of polyethylene films should be used, and therefore the slack film

layers can randomly scatter the incoming X-rays on the fast-rotating rollers. If a one-layered film is used for each thickness, the deviation could be minimized. Moreover, an optimal speed would be required in practical industry to reduce the errors depending on the rotation speeds.

A calibration-free real-time process monitoring of moving polyethylene films on a rotating roller was also demonstrated using strips of adhesive tapes placed onto the polyethylene film as a base to introduce the artificial variation in the thickness of the base film. As shown in Fig. 1 (c), several strips of adhesive tapes were spaced at a distance of approximately 2 cm between strips. Individual X-ray fluorescence and Compton scattering count rates obtained from X-ray spectra were plotted as a function of time in Fig. 8. In the case of Compton scattering signals in Fig. 8 (a) and (c), the changes in the count rates were not enough to detect the 0.16-mm-thick adhesive tapes on the polyethylene base film. Furthermore, considering the strong negative linear relation between the count rates of the fluorescence and film thickness, the abrupt drop of the count rates represents the detection of adhesive tapes. The roller machine was operated at speeds of 50 and 150 cm min⁻¹, and the time interval between two strips was approximately 2.5 and 0.8 s, with an actual tape width of 2.0 cm. The data confirmed the position and length of the tape strips. The thickness of the tape may also be evaluated with the decrease in count rates if the correlation between the intensity and thickness is re-evaluated using the tape on the polyethylene film. As expected from the sensitivity results in a lower thickness range presented in Fig. 7, the performance of X-ray fluorescence signals, shown in Fig. 8 (b) and (d), was superior to that using Compton scattering signals, shown in Fig. 8 (a) and (c).

4. Conclusion

A new simple non-contact and non-destructive real-time film thickness measurement technique has been proposed through the simulation of a field process dealing with thin flexible organic films and demonstrated by setting up a bench-top X-ray thickness measurement system. Our system is robust regardless of the movement of films on the rollers, and it is sensitive to organic films over a wide range of thickness using Compton scattering and fluorescence radiation. The use of reflectance signals from the film in close contact with the roller enables accurate thickness measurement, compared with other transmission measurement techniques with inherent errors due to the fluctuation of thin flexible films moving between rollers. Our study on the behavior of X-ray fluorescence and Compton scattering radiation made it possible to use the total count rate for the determination of film thickness on rotating rollers and calibration-free process monitoring dependent on the film thickness range. However, selecting X-ray signals in a certain thickness range should be considered, where the contribution of X-ray fluorescence or Compton scattering is not negligible. In such cases, the specific peak area of X-ray fluorescence or Compton scattering should be chosen depending on the respective signal intensities for the accurate thickness measurement. Under our experimental conditions, the measurement sensitivities of X-ray fluorescence signals are higher than those of Compton scattering signals. Our simple calibration-free technique can avoid tedious and time-consuming calibration procedures using standard samples before measurements. Thus, it optimizes and improves the measurement system, i.e., by adjusting the X-ray power, detector sensitivity, and geometry of the measurement system, making it a

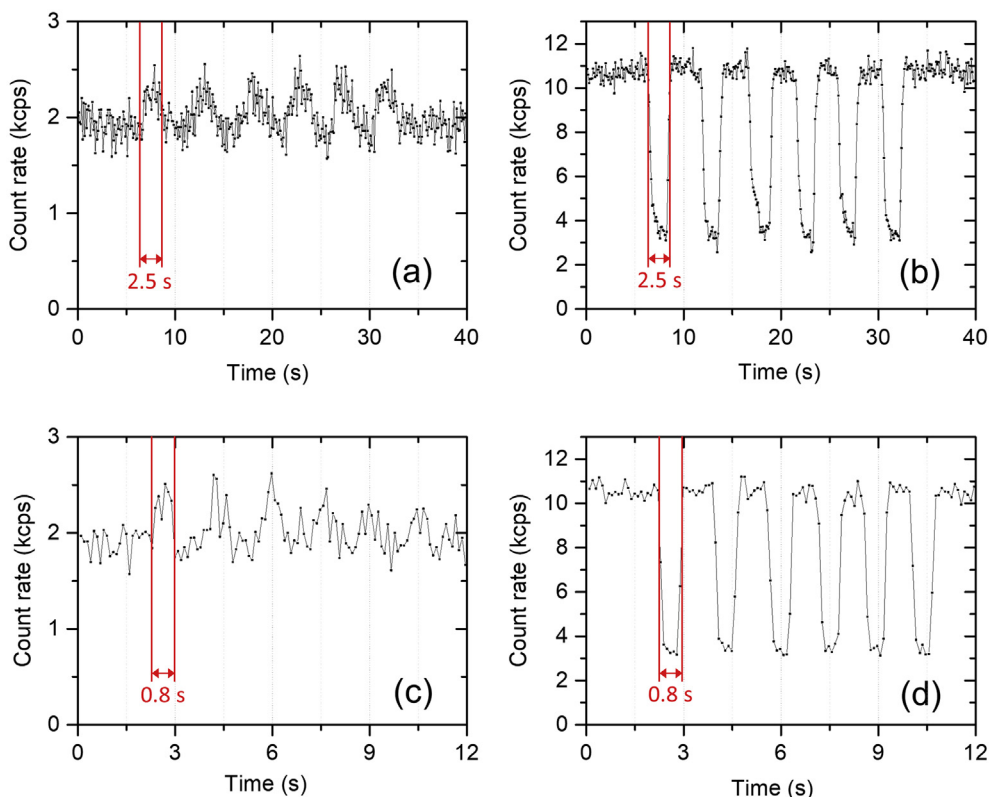


Fig. 8. Time–count rate curves for the calibration-free real-time process monitoring of polyethylene film on a roller moving at a constant speed of 50 and 150 cm min⁻¹. Data points show the count rates collected from (a) Compton scattering signals for 50 cm min⁻¹, (b) X-ray fluorescence signals for 50 cm min⁻¹, (c) Compton scattering signals for 150 cm min⁻¹, and (d) X-ray fluorescence signals for 150 cm min⁻¹ 2-cm-wide yellow adhesive tapes (shown in Fig. 1) were adhered onto the film at a distance of ca. 2 cm. Two red guide lines indicate the time span for a 2-cm distance. (For interpretation of the references to colour in this figure legend, the reader is referred to the Web version of this article.)

promising technique for the early fault detection in field processes. For practical industrial application, further tests are required with more wide range of experimental conditions such as rolling speeds, scattering angles, X-ray energies, type of organic materials, etc., in the future.

Declaration of competing interest

The authors declare that they have no known competing financial interests or personal relationships that could have appeared to influence the work reported in this paper.

Acknowledgements

This research was supported by the National Research Foundation of Korea funded by the Korean government (Ministry of Science and ICT) (grant nos. 2017M2A8A5014754 and 2019M1A7A1A02085179).

Appendix A. Supplementary data

Supplementary data to this article can be found online at <https://doi.org/10.1016/j.net.2020.09.018>.

References

- [1] K.A. Bakeev (Ed.), *Process Analytical Technology*, John Wiley & Sons, Chichester, UK, 2010, <https://doi.org/10.1002/9780470689592>.
- [2] S. Bordawekar, A. Chanda, A.M. Daly, A.W. Garrett, J.P. Higgins, M.A. LaPack, T.D. Maloney, J. Morgado, S. Mukherjee, J.D. Orr, G.L. Reid, B.-S. Yang, H.W. Ward, Industry perspectives on process analytical technology: tools and applications in API manufacturing, *Org. Process Res. Dev.* 19 (2015) 1174–1185, <https://doi.org/10.1021/acs.oprd.5b00088>.
- [3] S.W. Song, J. Kim, C. Eum, Y. Cho, C.R. Park, Y.-A. Woo, H.M. Kim, H. Chung, Hyperspectral Raman line mapping as an effective tool to monitor the coating thickness of pharmaceutical tablets, *Anal. Chem.* 91 (2019) 5810–5816, <https://doi.org/10.1021/acs.analchem.9b00047>.
- [4] J. Workman, D.J. Veltkamp, S. Doherty, B.B. Anderson, K.E. Creasy, M. Koch, J.F. Tatera, A.L. Robinson, L. Bond, L.W. Burgess, G.N. Bokerman, A.H. Ullman, G.P. Darsey, F. Mozayeni, J.A. Bamberger, M.S. Greenwood, Process analytical chemistry, *Anal. Chem.* 71 (1999) 121–180, <https://doi.org/10.1021/a1990007s>.
- [5] M.H. Ali, A. Rabhi, A. El Hajjaji, G.M. Tina, Real time fault detection in photovoltaic systems, *Energy Procedia* 111 (2017) 914–923, <https://doi.org/10.1016/j.egypro.2017.03.254>.
- [6] C.D. Dimitrakopoulos, D.J. Mascaro, Organic thin-film transistors: a review of recent advances, *IBM J. Res. Dev.* 45 (2001) 11–27, <https://doi.org/10.1147/rd.451.0011>.
- [7] C.D. Dimitrakopoulos, P.R.L. Malenfant, Organic thin film transistors for large area electronics, *Adv. Mater.* 14 (2002) 99–117, [https://doi.org/10.1002/1521-4095\(20020116\)14:2<99::AID-ADMA99>3.0.CO;2-9](https://doi.org/10.1002/1521-4095(20020116)14:2<99::AID-ADMA99>3.0.CO;2-9).
- [8] P. Peumans, A. Yakimov, S.R. Forrest, Small molecular weight organic thin-film photodetectors and solar cells, *J. Appl. Phys.* 93 (2003) 3693–3723, <https://doi.org/10.1063/1.1534621>.
- [9] P. Fenter, F. Schreiber, L. Zhou, P. Eisenberger, S. Forrest, In situ studies of morphology, strain, and growth modes of a molecular organic thin film, *Phys. Rev. B Condens. Matter* 56 (1997) 3046–3053, <https://doi.org/10.1103/PhysRevB.56.3046>.
- [10] P.V. Pesavento, K.P. Puntambekar, C.D. Frisbie, J.C. McKeen, P.P. Ruden, Film and contact resistance in pentacene thin-film transistors: dependence on film thickness, electrode geometry, and correlation with hole mobility, *J. Appl. Phys.* 99 (2006), 094504, <https://doi.org/10.1063/1.2197033>.
- [11] H. Jia, S. Gowrisanker, G.K. Pant, R.M. Wallace, B.E. Gnade, Effect of poly (3-hexylthiophene) film thickness on organic thin film transistor properties, *J. Vac. Sci. Technol. A Vacuum, Surf. Film.* 24 (2006) 1228–1232, <https://doi.org/10.1116/1.2202858>.
- [12] J.J. Allport, N.L. Brouwer, R.A. Kramer, Backscatter/transmission X-ray thickness gauge, *NDT Int.* 20 (1987) 217–223, [https://doi.org/10.1016/0308-9126\(87\)90244-6](https://doi.org/10.1016/0308-9126(87)90244-6).
- [13] O. Durand, V. Berger, R. Bisaro, A. Bouchier, A. De Rossi, X. Marcadet, I. Prévot, Determination of thicknesses and interface roughnesses of GaAs-based and InAs/AlSb-based heterostructures by X-ray reflectometry, *Mater. Sci. Semicond. Process.* 4 (2001) 327–330, [https://doi.org/10.1016/S1369-8001\(00\)00103-7](https://doi.org/10.1016/S1369-8001(00)00103-7).
- [14] C. Fiorini, A. Gianoncelli, A. Longoni, F. Zaraga, Determination of the thickness of coatings by means of a new XRF spectrometer, *X Ray Spectrom.* 31 (2002) 92–99, <https://doi.org/10.1002/xrs.550>.
- [15] M. Birkholz, *Thin Film Analysis by X-Ray Scattering*, John Wiley & Sons, Darmstadt, Germany, 2006.
- [16] M. Yasaka, X-ray thin-film measurement techniques, *Rigaku J* 26 (2010) 1–9.
- [17] H. Okada, M. Shibata, T. Echigo, S. Naka, H. Onnagawa, *Film Thickness Measuring Method and Measuring Apparatus for Organic Thin Film for Use in Organic Electroluminescence Device*, US6992781B2, 2006.
- [18] Y.S. Choi, J.-Y. Kim, S.B. Yoon, K. Song, Y.J. Kim, Determination of water content in silica nanopowder using wavelength-dispersive X-ray fluorescence spectrometer, *Microchem. J.* 99 (2011) 332–338, <https://doi.org/10.1016/j.microc.2011.06.003>.
- [19] J.Y. Kim, Y.S. Choi, Y.J. Kim, K. Song, S.H. Jung, E.M.A. Hussein, Thickness measurement of organic films using Compton scattering of characteristic X-rays, *Appl. Radiat. Isot.* 69 (2011) 1241–1245, <https://doi.org/10.1016/j.apradiso.2011.03.048>.
- [20] J.A. Bearden, A.F. Burr, Reevaluation of X-ray atomic energy levels, *Rev. Mod. Phys.* 39 (1967) 125–142, <https://doi.org/10.1103/RevModPhys.39.125>.
- [21] AMPTeK, X-123CdTe complete X-ray & gamma ray spectrometer, (n.d.), <https://www.amptek.com/products/cdte-x-ray-and-gamma-ray-detectors/x-123-cdte-complete-x-ray-gamma-ray-spectrometer-with-cdte-detector> (accessed August 23, 2020).
- [22] Y.S. Choi, J. Hwang, J.-Y. Kim, On-line and real-time analysis of moisture content in activated carbon powder by X-ray scattering technique, *Asian J. Chem.* 26 (2014) 4067–4069, <https://doi.org/10.14233/ajchem.2014.17715>.
- [23] H.A. van Sprang, M.H.J. Bekkers, Determination of light elements using x-ray spectrometry. Part I—analytical implications of using scattered tube lines, *X Ray Spectrom.* 27 (1998) 31–36, [https://doi.org/10.1002/\(SICI\)1097-4539\(199801/02\)27:1<31::AID-XRS245>3.0.CO;2-#](https://doi.org/10.1002/(SICI)1097-4539(199801/02)27:1<31::AID-XRS245>3.0.CO;2-#).